Affinity Pansharpening and Image Fusion

Stephen Tierney and Junbin Gao
School of Computing and Mathematics
Charles Sturt University
Bathurst, NSW 2795, Australia
{stierney, jbgao}@csu.edu.au

Yi Guo
Digital Productivity & Services Flagship
CSIRO
North Ryde, NSW 2113, Australia
yi.guo@csiro.au

***Abstract*—A novel framework for enhancing the resolution of a low-resolution multispectral or hyperspectral image using a high resolution panchromatic image or multispectral image is proposed in this paper. This framework can be further used to perform more general types of image fusion. To create the enhanced image, a convex objective function is minimised, which preserves both the pixel affinity learnt from the high resolution image and spectral information from the low resolution image. A fast approximation method is discussed. Quantitive and qualitative analysis against existing methods shows that our method is comparable to state of the art with faster running time and greater flexibility. MATLAB code for our proposed method and the compared methods are freely available in the FuseBox package[1].**

I. Introduction

In remote sensing multispectral (MS) and hyper spectral (HS) images are prolific. These images provide a high level of spectral detail. However these images are often of relatively low spatial resolution due to limited storage and bandwidth available onboard the satellites. Fortunately complementary images with high spatial resolution are available. One can use these high resolution images to enhance the apparent resolution of the high-spectral resolution images. This is the general task of image fusion. In remote sensing there are two typical image fusion tasks among others: pansharpening and Multi-spectral-Hyper-spectral fusion. In the pansharpening paradigm, a panchromatic (PAN) image is used to enhance a multispectral image. A panchromatic image is a high resolution, single channel image which captures a broad spectrum of light, often a majority of the spectrum captured in the multispectral image. These panchromatic images are captured at the same time as the MS imagery by the same satellite. Similarly one can use the MS image to enhance the HS image in MS-HS fusion. It is rarely the case that a single satellite captures both MS and HS images.

Pansharpening has attracted significant research attention. The most common class of techniques are called substitution techniques. Their framework consists of projecting the multi-spectral data to some intermediate representation then substituting some components with those in the panchromatic image then performing the reverse projection. Some examples of this kind of approach are Brovey [1][2], IHS [3][4][5][6], PCA [7][8] and Wavelet [9][10][11] transforms. For example in the PCA transform the principal components of the multispectral image are calculated and then the principal component with the highest variance is replaced with the panchromatic image. The inverse PCA is calculated to obtain a sharpened image.

[1] https://github.com/sjtrny/FuseBox

Substitution methods are destructive methods, meaning they directly replace multispectral image information with that from the panchromatic image. This has the potential to destroy spectral information which we want to preserve. Furthermore these methods are highly specialised to pansharpening and unable to perform MS-HS fusion, in contrast our proposed method can handle both problems.

More recent approaches fall into the class of "variational" methods, which take a cost function minimisation approach. These have been more successful at preserving spectral information but can often not transfer the structure of the high resolution image correctly. Prominent examples are P+XS [12] and AVWP [13]. More recently Chen et al. [14] proposed a new method, which has claimed to outperform all prior methods. Variational methods have the advantage that they could be adapted to the problem of MS-HS fusion. However this adaption has not been discussed in the literature.

A unique pan sharpening approach called Matting Model Pansharpening (MMP) was proposed in [15]. The authors treat the panchromatic image as the alpha channel and then estimate the foreground and background components from the multispectral image. The foreground and background components are upsampled to the panchromatic size and then recombined using the panchromatic image. There are significant problems with this approach. First the assumption that the multispectral image can be divided into foreground and background components is not realistic. Second the results are highly dependant on the ratio of the spatial resolution between the MS and panchromatic image. Third this approach is limited to pansharpening and cannot be used for general image fusion.

In the domain of MS-HS fusion a class of techniques based on matrix factorisation has dominated. These approaches rely on a decomposition approach [16][17][18][19][20]. They decompose the HS images into the combination of a dictionary of pure spectra of each material in the scene and their corresponding coefficients. Then the dictionary is used to represent the MS image in a similar factorisation model and the coefficients are learnt. The learnt dictionary and coefficients are recombined to produce the fused image. This approach is attractive because it considers the capture process of the MS and HS images and establishes a direct relationship. However the process can be time consuming and it may be the case that the optimisation procedures are non-convex.

Our proposed framework can be considered a variational fusion method. We softly penalise towards a solution using a convex objective function with the characteristics we desire i.e. high level of spatial detail and preservation of spectral informa-

978-1-4799-5409-4/14/$31.00 ©2014 IEEE

tion. The spatial detail from the high spatial resolution image is transferred by establishing a linear relationship between the high resolution image and the sharpened image. The spectral information is preserved by minimising the distance from the high-spectral resolution image and the sharpened image. Our method is general and allows for both pansharpening and MS-HS fusion. Furthermore we have a fast approximate solution, which is many times faster than existing variational methods.

II. Affinity Fusion Framework

In image fusion there are two requirements that we must fulfil to be successful:

- High resolution detail is transferred
- Spectral distortion is minimised

We propose a framework which achieves both these goals through the minimisation of a convex objective function. Let $\mathbf{A} = [\mathbf{a}_1, \mathbf{a}_2, \ldots, \mathbf{a}_D] \in \mathbb{R}^{N \times D}$ be the target image of N pixels and D channels, $\mathbf{M} \in \mathbb{R}^{N \times D}$ be the low resolution image, which has been upsampled to the same size as our target, and $\mathbf{P} \in \mathbb{R}^{N \times d}$ be the high resolution image with d channels. First to transfer detail from the high resolution image we use the following penalty

$$\sum_{c}^{D} \left(\sum_{i,j} W_{ij} (A_{ic} - A_{jc})^2 \right)$$

where W_{ij} is a learnt similarity coefficient from $\mathbf{P}$ and A_{ic} is the element of $\mathbf{A}$ at row i and column c. This penalty ensures that pixels that are similar in $\mathbf{P}$ are similar in $\mathbf{A}$ and consequently the high resolution structure is transferred.

Second we minimise the spectral distortion through the following penalty

$$\lambda \sum_{c}^{D} \left(\sum_{i}^{N} (A_{ic} - M_{ic})^2 \right)$$

where λ allows us to control how spectrally similar our sharpened image is to the original. Combining these penalties together we have our complete objective

$$\min_{\mathbf{A}} \sum_{c}^{D} \left(\sum_{i,j}^{N} W_{ij} (A_{ic} - A_{jc})^2 + \sum_{i}^{N} \lambda (A_{ic} - M_{ic})^2 \right) \quad (1)$$

This objective is the basis of our Affinity Fusion framework. Different from other methods we directly penalise for the desired characteristics of our fused or sharpened image. Furthermore this framework easily adapts from pansharpening to more general image fusion tasks since we are free to choose different schemes for calculating weights $\mathbf{W}$.

A. Solution

We begin discussing the solution to our objective by rewriting the objective into vector matrix notation

$$\min_{\mathbf{A}} \sum_{c}^{D} \left(\mathbf{a}_c^T \mathbf{L} \mathbf{a}_c + \lambda (\mathbf{a}_c - \mathbf{m}^c)^T (\mathbf{a}_c - \mathbf{m}^c) \right)$$

where $\mathbf{a}_c$ is channel c of the sharpened image, i.e. a column of $\mathbf{A}$. We can further rewrite the objective to

$$\min_{\mathbf{A}} \operatorname{Tr}(\mathbf{A}^T \mathbf{L} \mathbf{A}) + \lambda (\mathbf{A} - \mathbf{M})^T (\mathbf{A} - \mathbf{M}) \quad (2)$$

where $\mathbf{L} = \mathbf{D} - \mathbf{W}$, $\mathbf{W}$ encodes the weights W_{ij} between pixels and $\mathbf{D}$ is a diagonal matrix with $D_{ii} = \sum_j W_{ij}$. Since our objective function is convex w.r.t $\mathbf{A}$ we can find the global minimum by differentiating the objective, setting the derivative to 0 and solving for $\mathbf{A}$. This results in solving the following linear system

$$(\mathbf{L} + \lambda \mathbf{I})\mathbf{A} = \lambda \mathbf{M} \quad (3)$$

We provide an overview of the entire framework in Algorithm 1. Compared to other fusion techniques our framework has a straightforward implementation. Occasionally the spectra of our fused image may shift slightly, to correct this we match the histogram of the fused image with the low-resolution image.

Algorithm 1 Affinity Fusion

Require: $\mathbf{P}$, λ, $\widetilde{\mathbf{M}}$ - low resolution image
1: Upsample low resolution image to desired resolution
$$\mathbf{M} = \text{upsample}(\widetilde{\mathbf{M}})$$
2: Calculate Laplacian matrix
$$\mathbf{L} = \text{get\_laplacian}(\mathbf{P})$$
3: Solve the linear system
$$(\mathbf{L} + \lambda \mathbf{I})\mathbf{A} = \lambda \mathbf{M}$$
4: Match histograms to correct any distortion
$$\mathbf{A} = \text{imhistmatch}(\mathbf{A}, \mathbf{M})$$
5: **return** $\mathbf{A}$

III. Weights and Local Linear Model

Previously we have discussed the concept of affinity fusion from the perspective of a general framework. In this section we discuss a concrete choice of weights that reflect and enforce our assumptions on the relationship between PAN and MS images or MS and HS images. Keep in mind that this is not the only choice of weights that one may make. In the following section we show that our choice of weights affords a fast approximate solution to (1).

Our assumption is that a pixel in our sharpened imagery is a linear transformation of the high resolution image in a small window around that pixel. We discuss the case where we wish to sharpen a single channel image. Actually the solution for multi channel images is the same with the process applied to each channel independently. We express the local linear model as

$$a_i = \alpha p_i + \beta, \; \forall i \in w \quad (4)$$

where a_i is pixel i from $\mathbf{a}_c$, which is a single channel of the sharpened image (or column of $\mathbf{A}$), p_i is pixel i from $\mathbf{p}$, which is a single channel high resolution image (e.g. PAN), α, β are coefficients which we assume to be constant over the window w and i is the pixel in question.

From a physical perspective this linear model reflects the observation that the PAN image is a weighted sum of the MS images, when α is small. However this physical interpretation is not as accurate when performing MS-HS fusion since their is less spectral overlap between the images. Furthermore the local linear model ensures that $\mathbf{a}$ only has an edge if $\mathbf{p}$ has an edge as noted in [21]

In [22] they showed that the weights required to enforce the local linear model in our affinity fusion framework are given by

$$L_{ij} = \sum_{k:(i,j)\in w_k} \left(\delta_{ij} - \frac{1}{|w_k|} \left(1 + \frac{(p_i - \mu_k)(p_j - \mu_k)}{\sigma_k^2 + \frac{\epsilon}{|w_k|}} \right) \right)$$

where δ_{ij} is the Kronecker delta, μ_k and σ_k^2 are the mean and variance of $\mathbf{p}$ in window w_k, $|w_k|$ is the number of pixels in the window and ϵ is a small bias term that controls smoothness over the window. For the case where our high resolution image has multiple channels (e.g. MS-HS fusion) we change our linear model slightly to

$$a_i = \left(\sum_c \alpha_c P_{ic} \right) + \beta, \ \forall i \in w.$$

where P_{ic} is pixel i of channel c in the high resolution image (e.g. MS). Consequently the elements of $\mathbf{L}$ are given by

$$L_{ij} = \sum_{k:(i,j)\in w_k} \Bigg(\delta_{ij} - \frac{1}{|w_k|} \Bigg(1 + (\mathbf{P}(i,:) - \boldsymbol{\mu}_k)^T (\boldsymbol{\Sigma}_k + \frac{\epsilon}{|w_k|}\mathbf{I}_d)^{-1} (\mathbf{P}(j,:) - \boldsymbol{\mu}_k) \Bigg) \Bigg) \tag{5}$$

where $\mathbf{P}(i,:)$ is row i of $\mathbf{P}$, $\boldsymbol{\Sigma}_k$ is a $d \times d$ covariance matrix, $\boldsymbol{\mu}_k$ is a $d \times 1$ mean vector and $\mathbf{I}_d$ is a $d \times d$ identity matrix.

IV. Fast Approximation

The previously discussed method is costly in terms of

- Constructing the Laplacian $\mathbf{L}$
- Solving the linear system (3)

Fortunately the authors of [21] have provided a fast approximation that is equivalent to solving (2) with the previously discussed Laplacian. Instead of incorporating our spectral similarity constraint separately from the local linear model we include it directly. In other words we combine (4) with

$$m_i = a_i + n_i$$

where n_i is an unwanted feature like noise. In our case n_i actually accounts for some blurring effect i.e. $m_i = F(a_i)$, where F is a blurring function. However we model it as an additive effect rather than a permutation for simplicity. This suggests solving the following objective

$$F(\alpha, \beta) = \sum_c \sum_j \left(\sum_{i \in w_j} (\alpha_j p_i + \beta_j - m_i)^2 + \epsilon \alpha_j^2 \right)$$

Fortunately this objective has a closed form solution, requiring us to solve for α and β only:

$$\alpha_j = \frac{\frac{1}{|w_j|} \sum_{i \in w_j} p_i m_i - \mu_j \bar{m}_j}{\sigma_j^2 + \epsilon}$$

$$\beta_j = \bar{m}_j - \alpha_j \mu_j$$

where $\bar{m}_j$ is the mean of $\mathbf{m}$ in window j. After obtaining α and β we plug the values into the locally linear model (4) to compute a_i. Since the estimated value for pixel j will differ due to the overlapping nature of the windows we average all estimated values

$$a_i = \frac{1}{|w|} \sum_k \alpha_k p_i + \beta_k$$

It was shown in [21] that this is equivalent to solving our objective (2). Therefore we can skip both the construction of the laplacian $\mathbf{L}$ and solving the linear system (3). This greatly simplifies implementation and drastically improves running time and memory requirements.

For the case where our high resolution image has multiple channels the solution is

$$\boldsymbol{\alpha}_j = (\boldsymbol{\Sigma}_j + \epsilon \mathbf{I})^{-1} \left(\frac{1}{|w|} \sum_{i \in w_j} \mathbf{P}(i,:) m_i - \boldsymbol{\mu}_j \bar{m}_j \right)$$

$$\beta_j = \bar{m}_j - \boldsymbol{\alpha}_j^T \boldsymbol{\mu}_j$$

and the final sharpened image is given by

$$a_i = \bar{\boldsymbol{\alpha}}_j^T \mathbf{p}_i + \bar{\beta}_i$$

where $\bar{\boldsymbol{\alpha}}_j$ and $\bar{\beta}_i$ are the mean coefficient values over the local window. As before we can apply this to fusing multi channel images by applying this process to each channel independently.

V. Pansharpening Results

Our experiment consists of pansharpening 39 cropped images from original LANDSAT ETM+ (Enhanced Thematic Mapper Plus) images. This dataset is considerably larger in number of images than those used in previous works. Most other publications perform experiments on less than 10 images. Furthermore they do not provide overall image quality measures such as mean and median values. Instead they discuss statistics per image, which may not capture the full story.

We retained the multispectral bands 1-3 (RGB) and the panchromatic band 8. The multispectral bands are captured at a ground resolution of 30m^2 per pixel and the panchromatic band is captured at 15m^2 per pixel. The multispectral images were cropped to 400×400 pixels and the panchromatic image to 800×800 pixels. The source images are freely available from EarthExplorer [23].

Quantitive assessment for pan sharpening is difficult and there is much debate about testing methods [24][25]. The most common approach, and the one which we take, is to downsample both MS and PAN images by half and perform pansharpening. The result is then compared to the original MS image. We use two image quality metrics: Spectral Angle Mapper (SAM) [26] and the relative dimensionless global error in synthesis (ERGAS) [26]. There are many other metrics used in the remote sensing community, however we believe their properties are already represented by SAM and ERGAS.

The SAM metric measures the average spectral distortion in degrees between two images. SAM is defined as

$$\text{SAM}(\mathbf{a}, \mathbf{b}) = \arccos \left(\frac{\langle \mathbf{a}, \mathbf{b} \rangle}{\|\mathbf{a}\|_2 \cdot \|\mathbf{b}\|_2} \right)$$

	Brovey	IHS	PCA	Wavelet	P+XS	MMP	Affinity	Approximate
Mean	0.0085	0.0052	0.0051	0.0034	0.0042	**0.0020**	0.0028	0.0029
Median	0.0090	0.0051	0.0050	0.0034	0.0042	**0.0018**	0.0025	0.0027
Min	0.0050	0.0024	0.0026	0.0021	0.0026	**0.0013**	0.0020	0.0020
Max	.0113	0.0087	0.0081	0.0051	0.0056	**0.0036**	0.0047	0.0051

TABLE I: Statistics for ERGAS over the entire dataset. Smaller values are better. Bold values are minimums.

	Brovey	IHS	PCA	Wavelet	P+XS	MMP	Affinity	Approximate
Mean	7.3498	7.2231	6.6938	8.9797	8.8020	9.7924	**6.3517**	7.0964
Median	7.5747	7.4282	6.7351	9.6171	9.3646	10.7054	**6.0819**	6.2702
Min	1.6109	1.8388	2.1324	2.1336	2.2191	**1.0234**	2.0366	2.1967
Max	**9.1851**	9.2132	9.2360	11.9684	11.9504	13.4394	10.8614	13.6689

TABLE II: Statistics for SAM over the entire dataset. Smaller values are better. Bold values are minimums.

where $\mathbf{a}, \mathbf{b}$ are pixels from the fused image and reference image respectively. The final SAM score is the average of all SAM values over the image. The SAM only accounts for spectral distortion and ignores radiometric distortion, i.e. if $\mathbf{a}, \mathbf{b}$ are parallel but have different lengths their value will be the same. Since SAM measures the amount of spectral distortion we wish for the smallest value possible, with 0 meaning no spectral distortion.

The ERGAS metric attempts to provide a global picture quality measurement. It is defined as

$$\text{ERGAS}(\mathbf{A}, \mathbf{B}) = r100\sqrt{\frac{1}{D}\sum_{c=1}^{D}\left(\frac{\text{RMSE}(\mathbf{A}^c, \mathbf{B}^c)}{\bar{\mathbf{B}}^c}\right)^2}$$

where $\mathbf{A}, \mathbf{B}$ are the fused image and reference image respectively, r is the ratio of resolution between MS and PAN images (0.25 in this case) and D is the number of image channels. RMSE is the Root Mean Square Error which is defined as

$$\text{RMSE}(\mathbf{A}, \mathbf{B}) = \frac{1}{N}\sqrt{\sum_{i=1}^{N}(\mathbf{a}_i - \mathbf{b}_i)^2}$$

where N is the total number of pixels.

We compared our method to the following methods: Brovey, IHS, PCA, Wavelet, P+XS and MMP. MMP has claimed state of the art performance. More recently [14] has also claimed state of the art performance however we were unable to test against since the authors have not provided code. Quantitive results are available in Tables I and II. Under the ERGAS metric our affinity method and correspondingly our approximation were comparable to results from MMP. Under the SAM metric our affinity method had the lowest mean and median values, furthermore the maximum SAM value was lower than that of MMP.

Interestingly in our tests the SAM results for MMP did not reflect those found by the original authors. Although it had the lowest SAM value for one of the images it had the highest mean and median SAM scores across the entire dataset. Furthermore the SAM score does not always align with visual interpretation. For example the Brovey and IHS methods scored well but they exhibit the worst distortion visually. Some visual results can be found in Figures 1, 2, 3 and 4. In many cases the Brovey and IHS method swap colour values, most often green becomes blue and blue becomes green.

We noticed that the Wavelet method produces blocky results in the x-y directions and is unable to capture irregular edges in the image. The P+XS method produced more satisfactory results however there are often artifacts along the edges in the sharpened image. Our affinity method suffers from none of the previously described defects of other methods. It is able to transfer most edges from the PAN image, however it occasionally over smooths regions between edges. Similarly our fast approximation produced satisfactory results with only minor variation from the exact method. A comparison of the exact method and the approximation can be found in Figure 5.

VI. MS-HS Fusion Results

In this section we provide brief visual results for HS-MS affinity fusion. We were unable to compare to other existing methods [9][20][19][18][25] or provide quantitive analysis since they do not provide code for their methods. Results for affinity fusion can be found in Figure 6. In this test we use high resolution MS imagery to increase the resolution of low-resolution HS imagery. The data is from EarthExplorer [23] with the MS images from the ALI device and HS images from the Hyperion device aboard the EO-1 satellite. The bands closest to Red, Green and Blue wavelengths from the MS imagery was used to enhance a subset of the bands from the HS imagery. Visually the results are quite pleasing, with a high level of detail being transferred to the HS images.

VII. Conclusion and Future Work

We have proposed an evaluated a new pansharpening and general image fusion framework. This framework allows one to directly penalise towards the desired properties of structure transfer and spectral similarity. Quantitive and qualitative analysis against existing methods shows that our method is comparable to state of the art. When a particular weighting scheme is chosen we have an approximate scheme, which is significantly faster than the state of the art. Furthermore our framework is more flexible than state of the art pansharpening methods.

While we have proposed a successful framework there are areas of improvement remaining:

- Our spectral constraint is unrealistic. Instead of an additive noise model we should consider the permutation or blurring model.

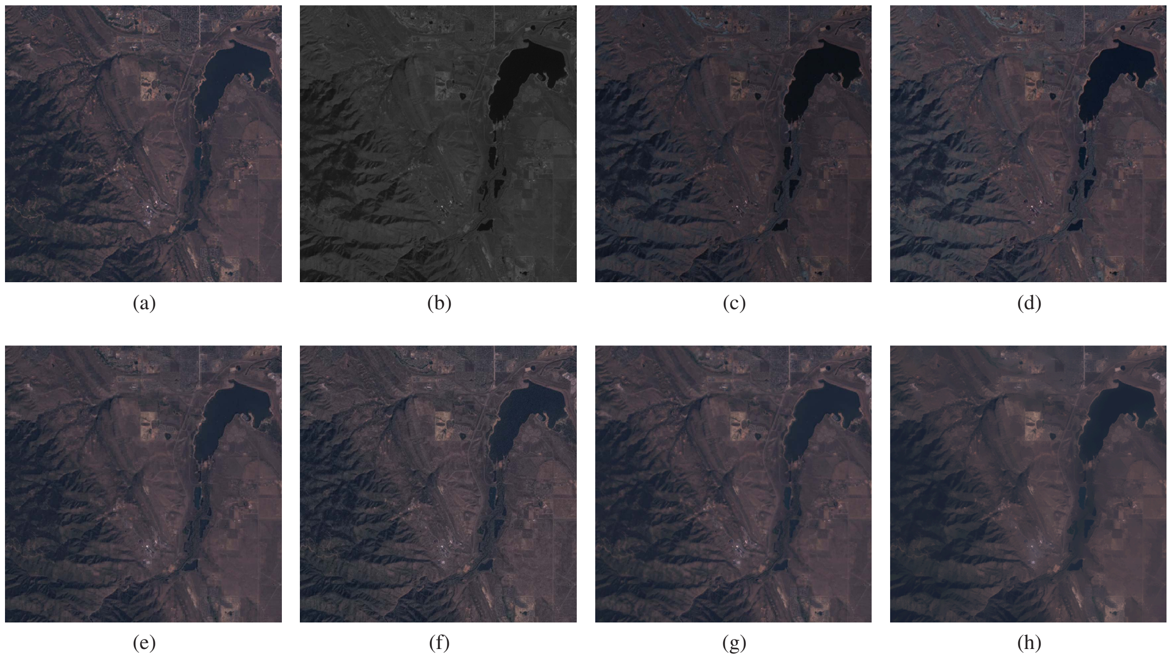

Fig. 1: Comparison of results from Pansharpening LANDSAT imagery. (a) Ground truth MS image, (b) Panchromatic image, (c)-(h) results of pansharpening from Brovey, IHS, Wavelet, P+XS, MMP, Affinity (ours) respectively.

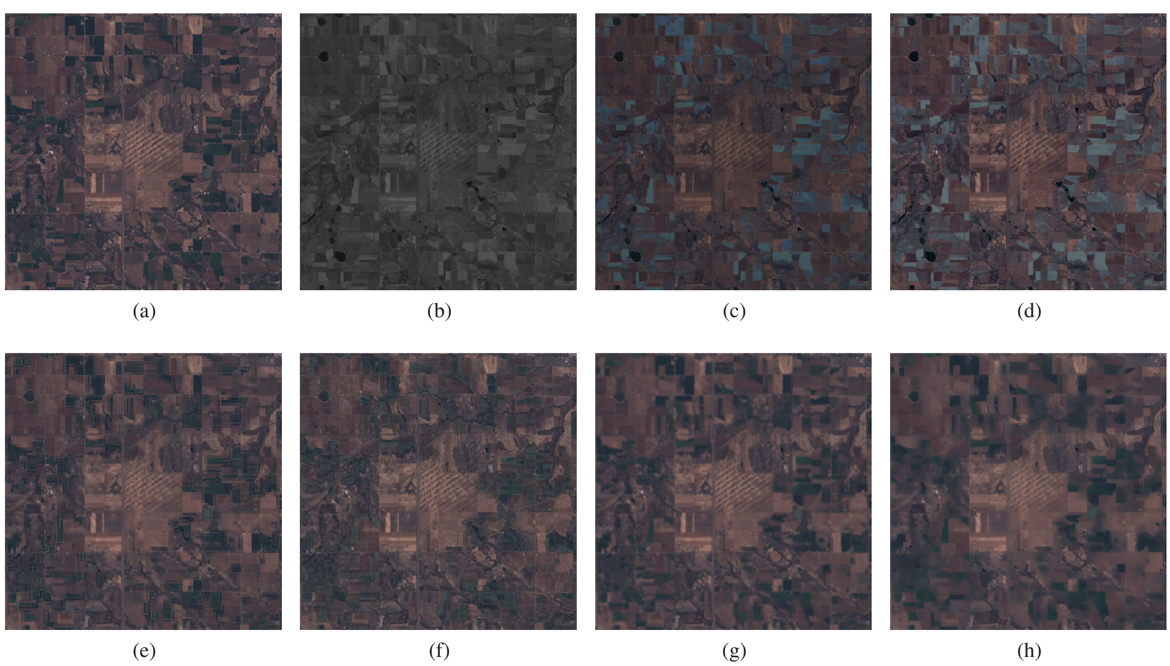

Fig. 2: Comparison of results from Pansharpening LANDSAT imagery. (a) Ground truth MS image, (b) Panchromatic image, (c)-(h) results of pansharpening from Brovey, IHS, Wavelet, P+XS, MMP, Affinity (ours) respectively.

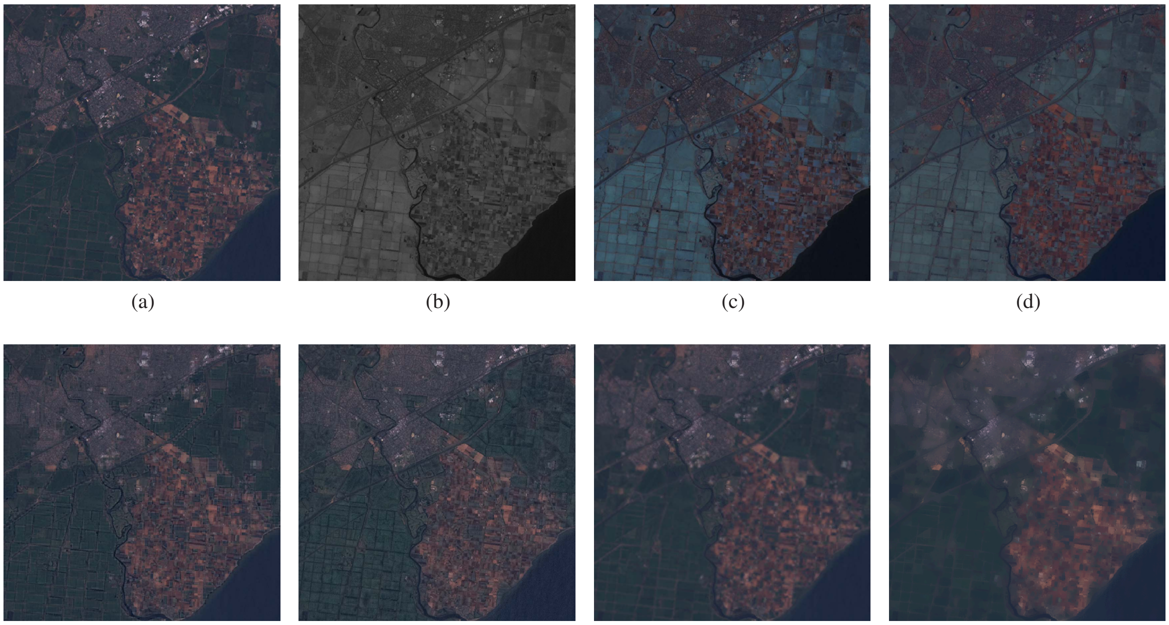

(a) (b) (c) (d)

(e) (f) (g) (h)

Fig. 3: Comparison of results from Pansharpening LANDSAT imagery. (a) Ground truth MS image, (b) Panchromatic image, (c)-(h) results of pansharpening from Brovey, IHS, Wavelet, P+XS, MMP, Affinity (ours) respectively.

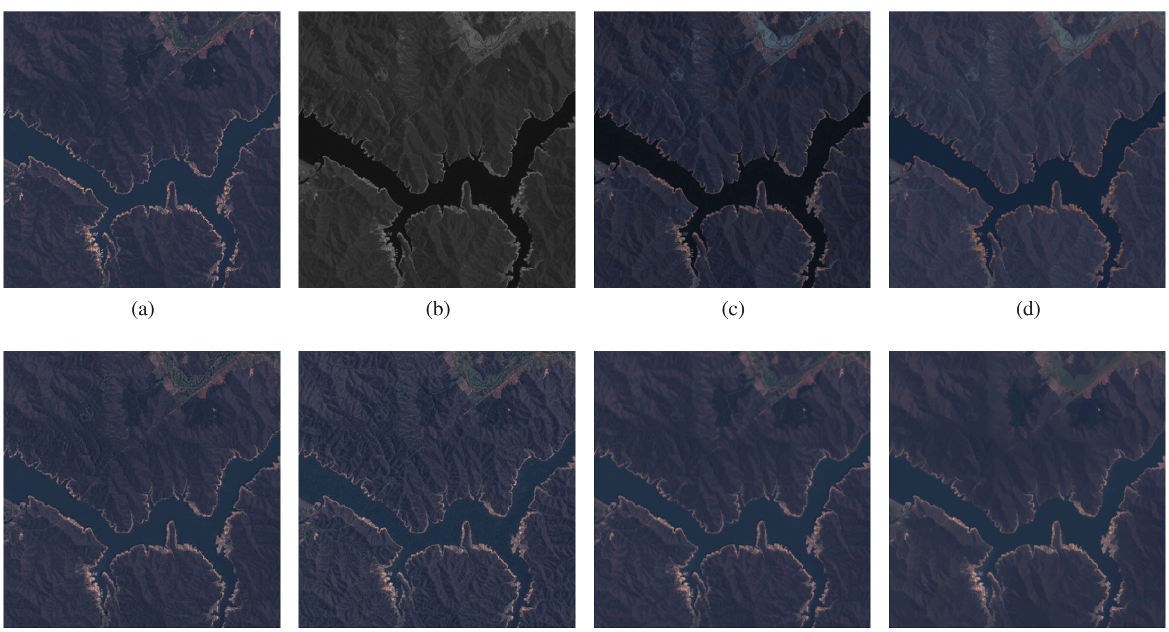

(a) (b) (c) (d)

(e) (f) (g) (h)

Fig. 4: Comparison of results from Pansharpening LANDSAT imagery. (a) Ground truth MS image, (b) Panchromatic image, (c)-(h) results of pansharpening from Brovey, IHS, Wavelet, P+XS, MMP, Affinity (ours) respectively.

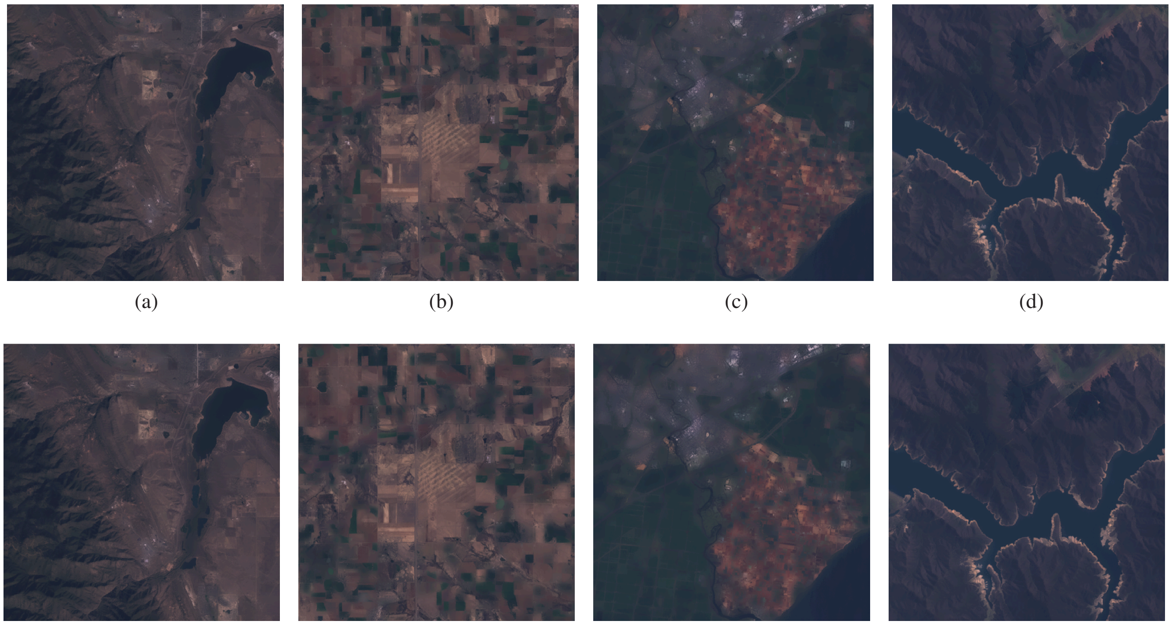

(a) (b) (c) (d)

(e) (f) (g) (h)

Fig. 5: Comparison of exact and approximate affinity pansharpening. (a)-(d) exact affinity method and (e)-(h) approximate method.

- The approximate solution we have proposed relies on the simplistic noise model. A new approximation method will need to be investigated if we change this model.

ACKNOWLEDGEMENT

This research was supported under Australian Research Council's Discovery Projects funding scheme (project number DP130100364) and partly supported under National Natural Science Foundation of China (project number 41371362). Imagery data available from the U.S. Geological Survey [23].

REFERENCES

[1] K.A. Kalpoma and J.-I. Kudoh, "Image fusion processing for ikonos 1-m color imagery," *Geoscience and Remote Sensing, IEEE Transactions on*, vol. 45, no. 10, pp. 3075–3086, Oct 2007.

[2] Alan R Gillespie, Anne B Kahle, and Richard E Walker, "Color enhancement of highly correlated images. ii. channel ratio and "chromaticity" transformation techniques," *Remote Sensing of Environment*, vol. 22, no. 3, pp. 343 – 365, 1987.

[3] W Joseph Carper, "The use of intensity-hue-saturation transformations for merging spot panchromatic and multispectral image data," *Photogrammetric Engineering and remote sensing*, vol. 56, no. 4, pp. 459–467, 1990.

[4] R. Haydn, G.W. Dalke, and J. Henke, "Application of the his color transform to the processing of multisensor data and image enhancemen," in *International Symposium on Remote Sensing of Arid and Semi-Arid Land*, 1982, pp. 599–616.

[5] JUNEM THORMODSGARD and JAYW FEUQUAY, "Larger scale image mapping with spot," *CNES, SPOT 1 Image Utilization, Assessment, Results p 1273-1279(SEE N 88-28346 22-43)*, 1988.

[6] Sheida Rahmani, Melissa Strait, Daria Merkurjev, Michael Moeller, and Todd Wittman, "An adaptive ihs pan-sharpening method," *Geoscience and Remote Sensing Letters, IEEE*, vol. 7, no. 4, pp. 746–750, 2010.

[7] Vijay P Shah, Nicolas H Younan, and Roger L King, "An efficient pan-sharpening method via a combined adaptive pca approach and contourlets," *Geoscience and Remote Sensing, IEEE Transactions on*, vol. 46, no. 5, pp. 1323–1335, 2008.

[8] Yun Zhang, "Understanding image fusion," *Photogrammetric engineering and remote sensing*, vol. 70, no. 6, pp. 657–661, 2004.

[9] Jorge Nunez, Xavier Otazu, Octavi Fors, Albert Prades, Vicenc Pala, and Roman Arbiol, "Multiresolution-based image fusion with additive wavelet decomposition," *Geoscience and Remote Sensing, IEEE Transactions on*, vol. 37, no. 3, pp. 1204–1211, 1999.

[10] Xavier Otazu, María González-Audícana, Octavi Fors, and Jorge Núñez, "Introduction of sensor spectral response into image fusion methods. application to wavelet-based methods," *Geoscience and Remote Sensing, IEEE Transactions on*, vol. 43, no. 10, pp. 2376–2385, 2005.

[11] Shutao Li, James T Kwok, and Yaonan Wang, "Using the discrete wavelet frame transform to merge landsat tm and spot panchromatic images," *Information Fusion*, vol. 3, no. 1, pp. 17–23, 2002.

[12] Coloma Ballester, Vicent Caselles, Laura Igual, Joan Verdera, and Bernard Rougé, "A variational model for p+ xs image fusion," *International Journal of Computer Vision*, vol. 69, no. 1, pp. 43–58, 2006.

[13] Michael Moeller, Todd Wittman, and Andrea L Bertozzi, "Variational wavelet pan-sharpening," *CAM Report*, pp. 08–81, 2008.

[14] Chen Chen, Yeqing Li, Wei Liu, and Junzhou Huang, "Image fusion with local spectral consistency and dynamic gradient sparsity," in *IEEE Conference on Computer Vision and Pattern Recognition (CVPR)*. IEEE, 2014.

[15] Xudong Kang, Shutao Li, and J.A. Benediktsson, "Pansharpening of remote sensing images with a matting model," in *Geoscience and Remote Sensing Symposium (IGARSS), 2013 IEEE International*, July 2013, pp. 1226–1229.

[16] Bo Huang, Huihui Song, Hengbin Cui, Jigen Peng, and Zongben Xu, "Spatial and spectral image fusion using sparse matrix factorization," *Geoscience and Remote Sensing, IEEE Transactions on*, vol. 52, no. 3, pp. 1693–1704, 2014.

[17] Naveed Akhtar, Faisal Shafait, and Ajmal Mian, "Sparse spatio-spectral representation for hyperspectral image super-resolution," in *Computer Vision–ECCV 2014*, pp. 63–78. Springer, 2014.

[18] N. Yokoya, T. Yairi, and A. Iwasaki, "Coupled nonnegative matrix factorization unmixing for hyperspectral and multispectral data fusion," *Geoscience and Remote Sensing, IEEE Transactions on*, vol. 50, no. 2, pp. 528–537, Feb 2012.

[19] Zhou Zhang, Zhenwei Shi, and Zhenyu An, "Hyperspectral and panchromatic image fusion using unmixing-based constrained nonneg-

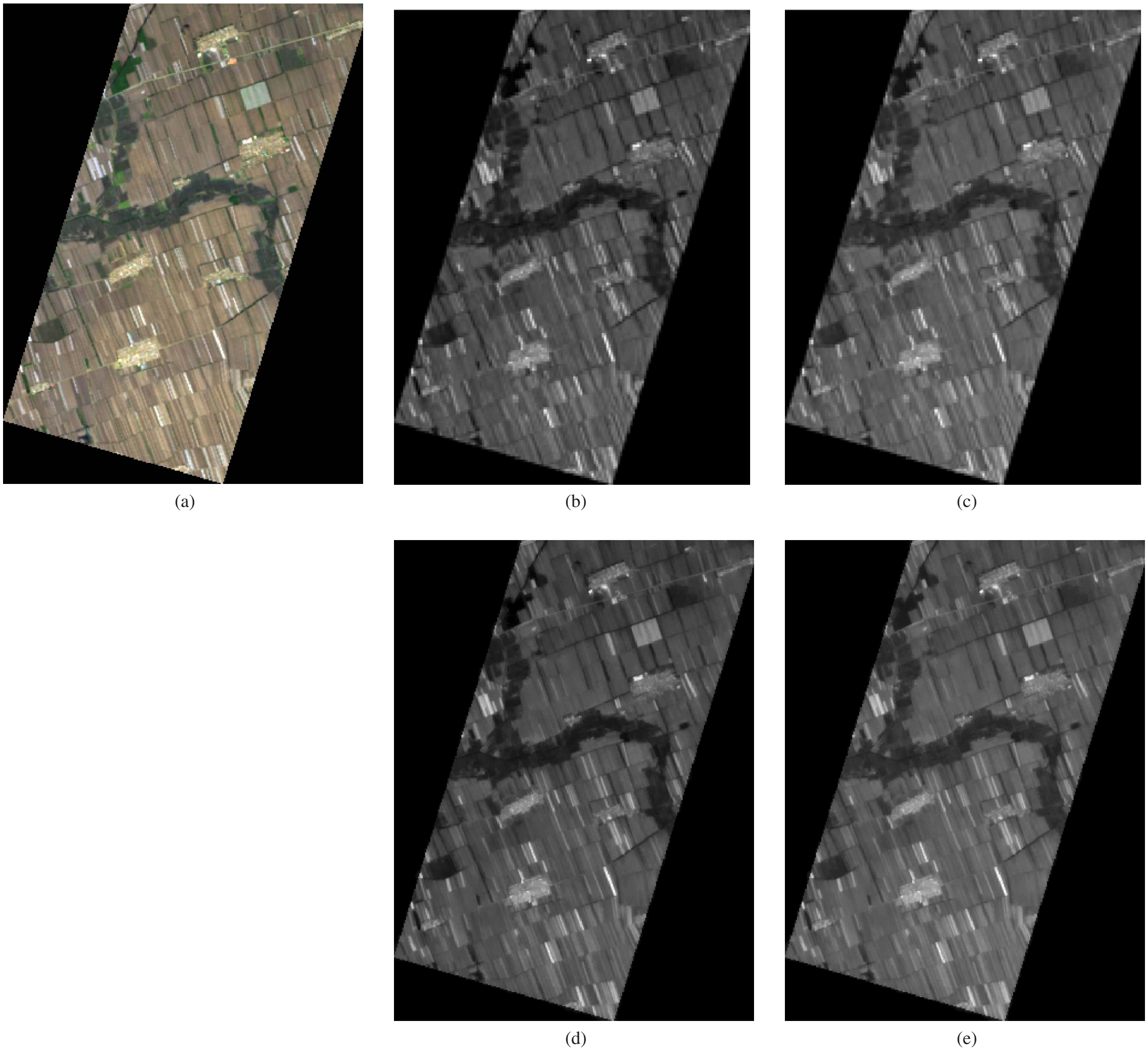

Fig. 6: Example results for MS-HS fusion from EO-1 data. (a) MS image, (b),(c) low-resolution single band HS images and (d),(e) fused images with higher resolution.

ative matrix factorization," *Optik - International Journal for Light and Electron Optics*, vol. 124, no. 13, pp. 1601 – 1608, 2013.

[20] Quan Chen, Zhenwei Shi, and Zhenyu An, "Hyperspectral image fusion based on sparse constraint {NMF}," *Optik - International Journal for Light and Electron Optics*, vol. 125, no. 2, pp. 832 – 838, 2014.

[21] Kaiming He, Jian Sun, and Xiaoou Tang, "Guided image filtering," *Pattern Analysis and Machine Intelligence, IEEE Transactions on*, vol. 35, no. 6, pp. 1397–1409, 2013.

[22] Anat Levin, Dani Lischinski, and Yair Weiss, "A closed-form solution to natural image matting," *IEEE Transactions on Pattern Analysis and Machine Intelligence*, vol. 30, no. 2, pp. 228 – 242, February 2008.

[23] United States Geological Survey, "Earthexplorer http://earthexplorer.usgs.gov/," .

[24] Qian Du, N.H. Younan, R. King, and V.P. Shah, "On the performance evaluation of pan-sharpening techniques," *Geoscience and Remote Sensing Letters, IEEE*, vol. 4, no. 4, pp. 518–522, Oct 2007.

[25] Mufit Cetin and Nebiye Musaoglu, "Merging hyperspectral and panchromatic image data: qualitative and quantitative analysis," *International Journal of Remote Sensing*, vol. 30, no. 7, pp. 1779–1804, 2009.

[26] L. Alparone, L. Wald, J. Chanussot, C. Thomas, P. Gamba, and L.M. Bruce, "Comparison of pansharpening algorithms: Outcome of the 2006 grs-s data-fusion contest," *Geoscience and Remote Sensing, IEEE Transactions on*, vol. 45, no. 10, pp. 3012–3021, Oct 2007.